HISTOGRAM MATCHING SEISMIC WAVELET PHASE ESTIMATION

A Thesis

Presented to

the Faculty of the Department of Earth and Atmospheric Sciences

University of Houston

In Partial Fulfillment

of the Requirements for the Degree

Master of Science

By

Jiangbo Yu

May 2012

HISTOGRAM MATCHING SEISMIC WAVELET PHASE ESTIMATION

Jiangbo Yu

APPROVED:

Dr. John Castagna, Chairman
Department of Earth and Atmospheric Sciences

Dr. Evgeny Chesnokov
Department of Earth and Atmospheric Sciences

Dr. Donald Kouri
Department of Chemistry

Dean, College of Natural Sciences and Mathematics

Acknowledgements

I would like to thank Dr. John Castagna, not only for offering me the opportunity to work with him on this project, but also for his continued guidance and advice throughout its duration. His encouragement and unique knowledge were extremely helpful in completing my research.

I want to thank my committee members, Dr. Evgeny Chesnokov and Dr. Donald Kouri, for their guidance and support throughout the course of this research.

Thanks also go to my friends and the department faculty and staff for making my time at University of Houston a great expericence.

Finally, thanks to my mother and father for their encouragement and to my fiance for her patience and love.

HISTOGRAM MATCHING SEISMIC WAVELET PHASE ESTIMATION

An Abstract of a Thesis

Presented to

the Faculty of the Department of Earth and Atmospheric Sciences

University of Houston

In Partial Fulfillment

of the Requirements for the Degree

Master of Science

By

Jiangbo Yu

May 2012

Abstract

The seismic wavelet phase can be estimated by histogram matching between seismically inverted reflectivity and well log reflectivity. Histogram matching is based on the convolutional model and assumes the wavelet is constant. If these assumptions are correct, the method is able to recover the wavelet phase information from seismic data with an error of less than 20 degrees if given high-quality seismic data and accurate wavelet amplitude spectrum estimation. As compared to maximum kurtosis phase estimation, this method doesn't need a super-Gaussian-distribution assumption for the reflectivity series. The model tests show that a large amount of data is needed to stabilize the kurtosis phase estimation method. For 1000-sample traces, kurtosis phase estimation can estimate phase with an error of less than 20 degrees for only 57 of 100 tests. For 2000-sample traces, this number increases to 60 out of 100, and 74 out of 100 for the 4000-sample traces; whereas the accuracy of histogram matching phase is relatively insensitive to trace lengths of this order. Compared to the optimum Wiener filter wavelet estimation methods, the histogram matching method is not sensitive to an inaccurate timing relationship between seismic data and well logs. A high-quality seismic dataset with high S/N is preferred to ensure an accurate phase estimation output. In addition, reflectivity skewness can be used to help identify polarity of the seismic wavelet.

Contents

List of Figures

List of Tables

Chapter 1

Introduction and Background

1.1 Introduction

1.1.1 Motivations for Wavelet Phase Estimation

The seismic wavelet plays an important role in various aspects of seismic analysis. From the point of view of seismic data processing, a wavelet must be reliably estimated so that it can generally be deconvolved or shaped to some desired output with a digital filter, and thus approximate the reflectivity series. The data resolution is improved (i.e. improve the ability to separate two features that are close together, from Sheriff, 2002) by increasing the sharpness of the seismic reflection. For a seismic interpreter, knowledge of the wavelet character and phase is important since any phase ambiguities may result in incorrect identification of low-and high- impedance layers in a seismic section (Brown, 2004).

Different methods have been developed and applied to estimate and remove the

wavelet (Robinson, 1957; Anstey 1958; Treitel and Robinson, 1967; White and O'Brien 1974; Ziolkowski, 1991). However these methods focus more on the amplitude estimation of the wavelet and leave the phase to the assumption that the seismic wavelet is either minimum phase or zero phase. Since this assumption is not always valid and both amplitude and phase are needed to characterize a wavelet, a reliable wavelet phase estimation method is necessary.

1.1.2 Approaches to the Problem

Various approaches to phase determination have been proposed and applied. We will consider three different methods which are based on different philosophies.

The traditional method of phase estimation is to use the optimum Wiener filter required to produce the seismogram from a given reflectivity series obtained from well logs.

A kurtosis based phase estimation method has been recently studied by Van der Baan et al. (2010), Van der Baan and Fomel (2009), Edgar (2008,) Van der Baan and Pham (2008) and Van der Baan (2008) following the work of Wiggins (1978). This method allows phase estimation without well logs.

In this thesis a hybrid method is developed, whereby the well log reflectivity is used to establish the distribution of reflection coefficients, and the wavelet phase that upon reflectivity inversion most closely reproduces this distribution is selected.

1.2 Background

1.2.1 Phase

Phase is a technical term that has been extensively used across different disciplines with various meanings. Before discussing phase estimation methods, it is necessary and helpful to clarify the meanings of phase, specifically the top four senses in seismic research and application (Liner, 2002).

Phase of the complex number. Phase is mathematically defined with the complex number:

$$z = x + iy \tag{1.1}$$

where x and y are real numbers and i is the square root of negative one. A complex number could also be written as:

$$z = Ae^{i\theta} \tag{1.2}$$

where A is the amplitude, and θ is the phase of the complex number z. From a geometric point of view, z is a point in a coordinate plane, A is the distance from the origin to the point and θ is the angle measured counterclockwise from the horizontal axis as demonstrated in Figure 1.1.

Phase of the wavefield. Assuming a simplest situation with a point source in an infinite homogeneous isotropic medium, the wavefield generated by the point source could be mathematically expressed as:

$$f = \frac{1}{r}\delta(t - r/c) \tag{1.3}$$

where r is the distance from the source, t is the time since the source started, and c is the speed of wave propagation. The function $\delta\,()$ is called the delta function

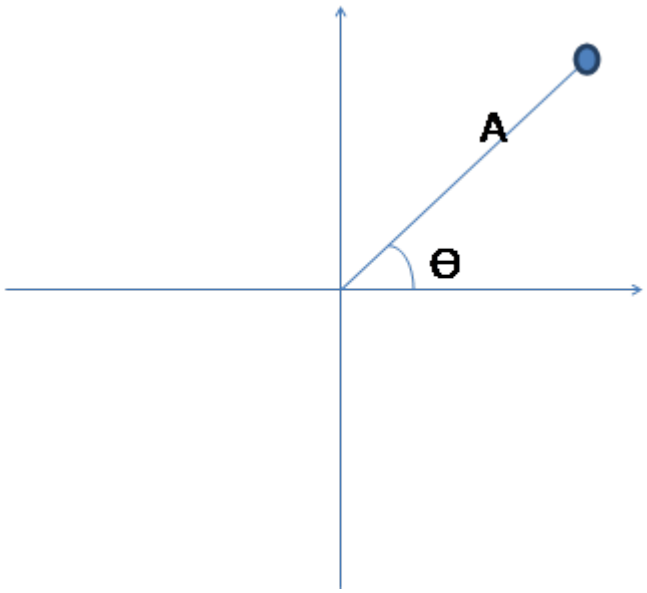

Figure 1.1: A plot illustrating amplitude and phase of a complex number in a coordinate plane.

which describes the wavefront location. Applying a Fourier transform over time, the wavefield could be expressed in frequency domain as:

$$f = \frac{1}{r} e^{iwr/c} \tag{1.4}$$

which is in the familiar form $Ae^{i\theta}$. So we see the wavefront location $(t - r/c)$ can be thought of as the phase of the wavefield.

Phase of a time series. The phase of a time series, such as a wavelet, is a description of its relative shape and time position (Badley, 1985). Applying a Fourier transform to a time series generates a phase spectrum which is a measure of how the timings of various frequency components of the time series relate (Simm and White, 2002). It might be zero phase, or minus 30° or it might change with frequency. A wrapped phase spectrum will stay bounded between $-180°$ and $+180°$

since it is defined by an inverse tangent function. For the fully processed seismic data, the phase of the wavelet is assume to be zero for all frequencies which gives a symmetric wavelet, centered on the reflection from an acoustic impedance boundary, thus making it the most desirable wavelet for interpretation. This kind of phase is what we are trying to estimate from seismic data in this thesis. Figure 1.2 and Figure 1.3 show two examples of how phase spectrum relates to the timing of wavelet: a linear phase shift is equivalent to a constant time shift, and a constant phase shift over all the frequencies will change the shape of a wavelet. In particular, a 90-degree phase shift converts a symmetric wavelet to an antisymmetric wavelet, while a 180-degree phase shift changes its polarity (Yilmaz 2001).

Minimum, mixed and maximum phase. Minimum, mixed, and maximum phase are used to describe casual signals. It has nothing to with the quantity of phase, saying 180 degrees is the maximum phase or zero phase is the minimum phase. In this case, phase indicates that the energy in the causal wavelet has a certain delay from the beginning of the wavelet. A minimum phase wavelet has minimum delay, a mixed phase wavelet builds up in the middle and a maximum phase wavelet builds up at the end as shown in Figure 1.4.

1.2.2 The Convolutional Model of the Seismogram

This study is based on the classic convolutional model of the seismogram. The recorded seismogram $s(t)$ can be modeled as the convolution of the Earth's impulse response or reflectivity $r(t)$ with the seismic wavelet $w(t)$ plus recorded noise $n(t)$:

$$s(t) = w(t) * r(t) + n(t) \tag{1.5}$$

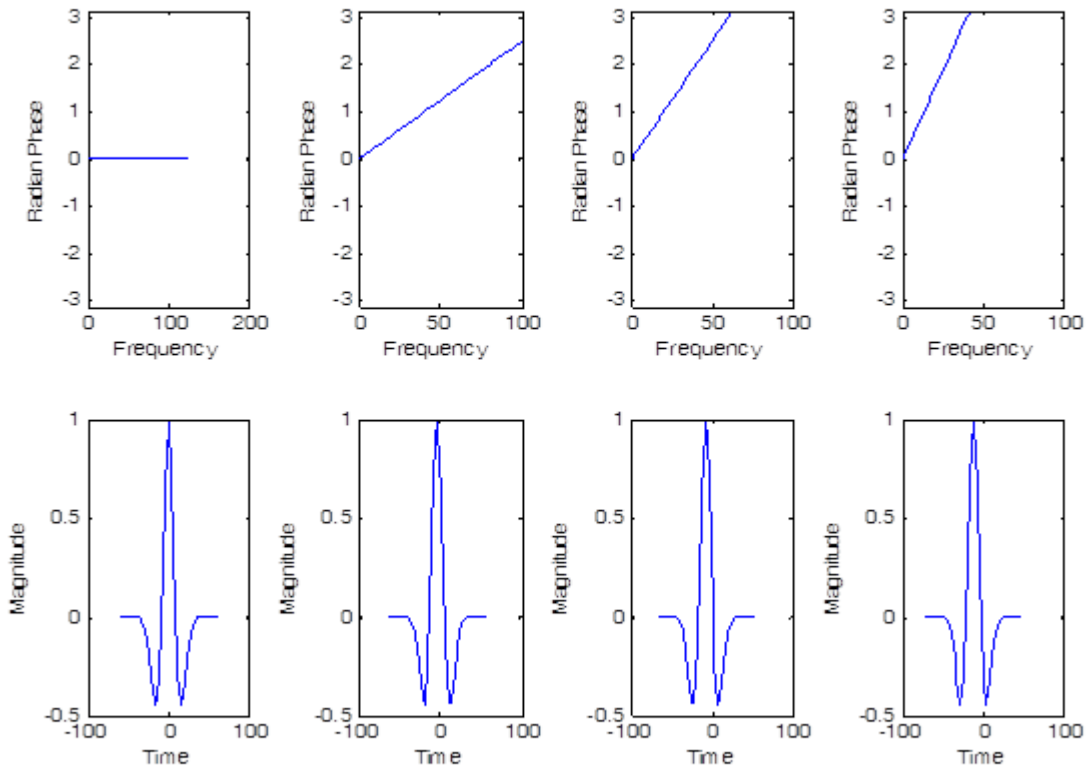

Figure 1.2: Linear phase shifts are applied to shift the wavelet in time without changing its shape. The slope of the linear phase function is related to the time shift (modified after Yilmaz 2001).

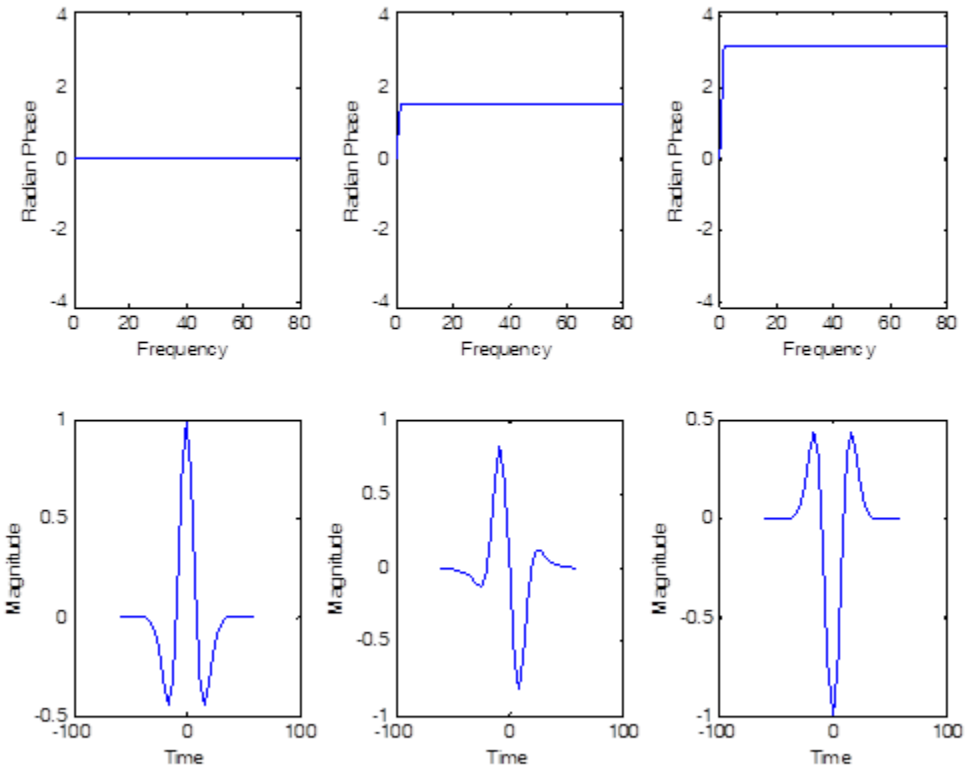

Figure 1.3: Starting with the zero-phase wavelet (a), its shape is changed by applying constant phase shift. A 90-degree phase shift converts the zero-phase wavelet to an antisymmetric wavelet (b), while a 180-degree phase shift reverses its polarity (c) (modified after Yilmaz 2001).

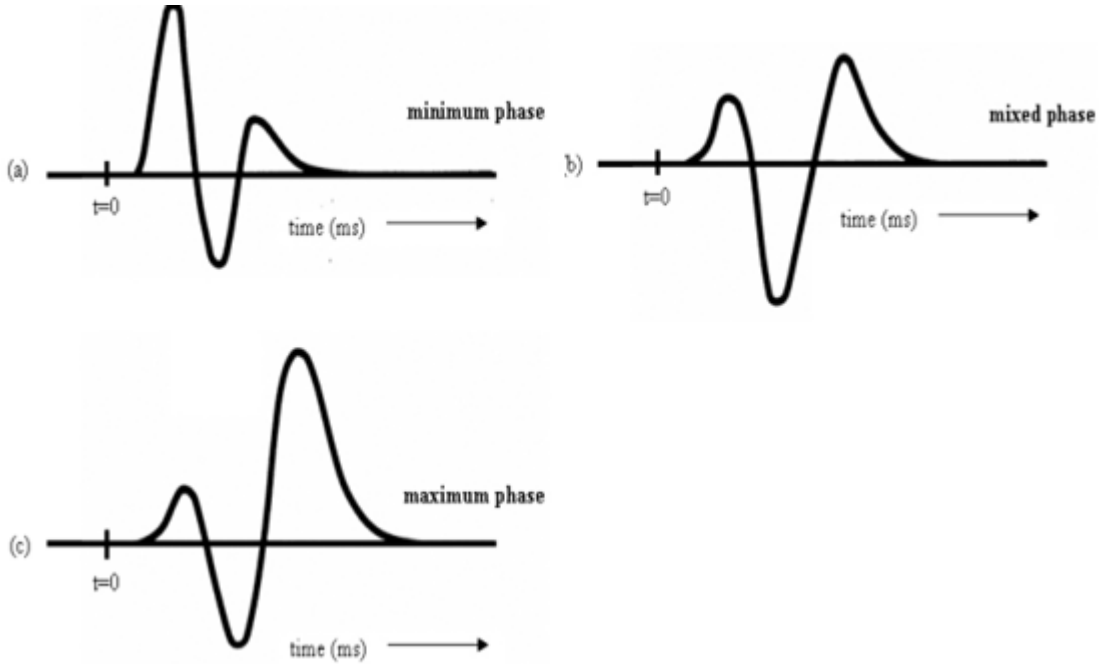

Figure 1.4: (a) Minimum phase wavelet, (b) mixed phase wavelet, (c) maximum phase wavelet (Liner 2004).

This impulse response of the Earth is what would be recorded if the wavelet were just a delta function or spike. A number of assumptions are made for this convolutional model (Yilmaz 2001), therefore, they are also applied to this whole study.

Assumption 1 The Earth is comprised of horizontally deposited lithological layers that exhibit constant velocity.

Assumption 2 An impulsive seismic source generate a compressional pressure wave that impinges on lithological layers at normal incidence, therefore, no shear waves are generated.

Assumption 3 The wavelet does not change as it travels in the Earth's sub-surface; that is to say, the seismic source signature is stationary. So the constant

wavelet phase estimation will be studied.

Assumption 4 The random noise component in a recorded seismogram is zero or can essentially be reduced to zero by processing.

Assumption 5 Reflectivity is a random process. This implies that the seismogram has the characteristics of the seismic wavelet in that their autocorrelations and amplitude spectra are similar.

Certain other assumptions for each specific method will be further discussed in the next chapter.

1.2.3 Inverse Filtering

If there is a filter $a(t)$ such that $r(t) = a(t) * s(t)$, that is to say, to recover the reflectivity by filtering seismic data with $a(t)$, then the convolutional model of the Earth becomes $s(t) = w(t) * a(t) * s(t)$. The noise component is neglected here. Simplifying this equation by eliminating $s(t)$ gives

$$w(t) * a(t) = \delta(t) \tag{1.6}$$

It implies $a(t) = \delta(t) * w'(t)$, where $w'(t)$ is the inverse wavelet. So the inverse of the seismic source signature is the operator required to recover the Earth's impulse response from a recorded seismogram. So one way to perform deconvolution is to transform the seismic trace and known wavelet to the frequency domain and divide. Taking into account the noise, the inverse filter in frequency domain is given by:

$$A(f) = \frac{\overline{W(f)}}{|W(f)|^2 + \sigma_n^2} \tag{1.7}$$

where capitalized letters represent their lower-case time-domain counterparts in the

frequency domain, σ_n^2 is the stabilization factor and the bar indicates a complex conjugate.

1.2.4 Optimum Wiener Filters

The optimum Wiener filter is designed by solving so-called normal equations:

$$\begin{pmatrix} r_0 & r_1 & r_2 & \cdots & r_{n-1} \\ r_1 & r_0 & r_1 & \cdots & r_{n-2} \\ r_2 & r_1 & r_0 & \cdots & r_{n-3} \\ \vdots & \vdots & \vdots & \ddots & \vdots \\ r_{n-1} & r_{n-2} & r_{n-2} & \cdots & r_0 \end{pmatrix} \begin{pmatrix} a_0 \\ a_1 \\ a_2 \\ \vdots \\ a_{n-1} \end{pmatrix} = \begin{pmatrix} g_0 \\ g_1 \\ g_2 \\ \vdots \\ g_{n-1} \end{pmatrix} \tag{1.8}$$

Here r_i, a_i, and g_i, $i = 0, 1, 2, \cdots, n-1$ are the auto-correlation lags of the input signal, the Wiener filter coefficients, and the cross-correlation lags of the desired output with the input signal, respectively. The optimum Wiener filter is optimum in that the least-square error between the actual and desired outputs is minimum. So when the input signal and desired output is given, for example, the reflectivity as input and seismogram as output, the optimum Wiener filter could be designed to minimize the difference between input and desired output, giving a wavelet estimation in this example. The Wiener-Levinson algorithm could be exploited to solve the equation for the filter coefficients.

Chapter 2

Statistical Signal Analysis

2.1 Zero-phase Wavelet Estimation

A zero-phase wavelet could be extracted from seismic data. The amplitude of a wavelet is based on the windowed auto-correlation of the seismic data. Auto-correlation is a measure of similarity between the events on a time series at different time positions. It is a running sum given by the expression

$$c_\epsilon(\tau) = \frac{1}{N} \sum_{t=0}^{N-1} e_t e_{t+z} \tag{2.1}$$

where τ is time lag. A random time series is an uncorrelated series. Therefore,

$$\begin{aligned} c_\epsilon(\tau) &= 0, \tau \neq 0 \\ c_\epsilon(0) &= r_0 = constant \end{aligned} \tag{2.2}$$

Equation 2.2 states that auto-correlation of a perfect random series is zero at all lags except at zero lag.

Consider the z-transform of the convolutional model in equation 1.3:

$$S(z) = W(z)R(z) \tag{2.3}$$

By putting $1/z$ in place of z and taking the complex conjugate, we get

$$\overline{S}(1/z) = \overline{W}(1/z)\overline{R}(1/z) \tag{2.4}$$

where the bar denotes the complex conjugate. By multiplying both sides of equations 2.3 and 2.4, we get

$$S(z)\overline{S}(1/z) = [W(z)R(z)]\left[\overline{W}(1/z)\overline{R}(1/z)\right] \tag{2.5}$$

By rearranging the right side,

$$S(z)\overline{S}(1/z) = \left[W(z)\overline{W}(1/z)\right]\left[R(z)\overline{R}(1/z)\right] \tag{2.6}$$

Finally,by definition,equation 2.6 yields

$$c_s = c_w * c_r \tag{2.7}$$

where c_s, c_w, and c_r are the auto-correlations of the seismogram, seismic wavelet, and impulse response, respectively. Based on the white reflectivity series assumption (equation 2.2), we have

$$c_s = c_0 c_w \tag{2.8}$$

Equation 2.8 states that the auto-correlation of the seismogram is a scaled version of that of the seismic wavelet.

Do the Fourier transform in equation 2.8

$$|S(\omega)|^2 = c_0^2|W(\omega)|^2 \tag{2.9}$$

so the zero-phase wavelet can be extracted by (1) averaging the amplitude spectra of all traces in each time window and (2) multiplying the averaged window in the time domain by a Hanning taper for enhanced robustness, while (3) ensuring that the amplitude at the Nyquist frequency remains zeros. The Hanning filter smooths the spectral estimate, thus ensuring extra robustness and it allows for the inclusion of any a priori information on the expected wavelet length (Van der Baan 2008).

2.2 Kurtosis and Central Limit Theorem

In statistics, kurtosis is a fourth-order statistic which measures the sharpness of the probability distribution of a real-valued random variable. It quantifies the deviation of a probability distribution from Gaussian distribution (Figure 2.1). Negative kurtosis describes a sub-Gaussian distribution, while positive kurtosis indicates a super-Gaussian distribution. A normal distribution will, therefore, have zero kurtosis. (Edgar 2008). It is commonly approximately by:

$$kurt(x) = n\frac{\sum x^4(t)}{[\sum x^2(t)]^2} - 3 \tag{2.10}$$

where $x(t)$ is a discrete time series, n is the number of time samples and t is the discrete time (Van der Baan, 2008). As a higher-order statistic, kurtosis holds information about the wavelet phase (Sacchi and Ulrych, 2000), so it is an obvious choice of norm for statistical wavelet approximation (Longbottom et al., 1988).

The Central Limit Theorem states that the sum of a large number of independent and identically distributed random variables will be approximately normally distributed if the random variables have a finite variance (Halmos, 1944). Applying

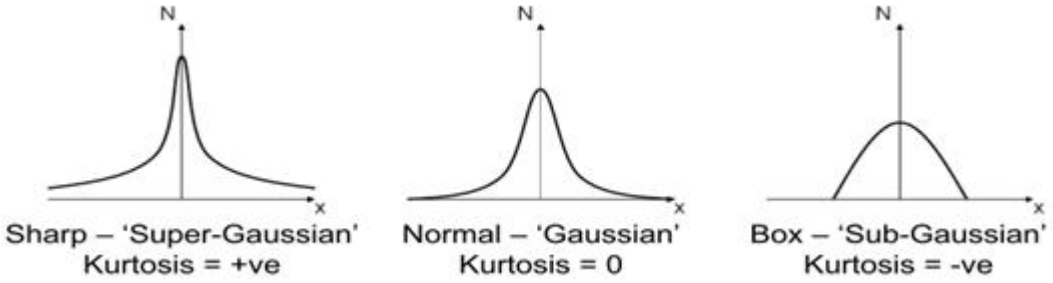

Figure 2.1: The relationship between Kurtosis and Gaussian distribution (Edgar 2008).

this to the convolutional model, the seismogram is less white and more Gaussian compared to the white reflectivity series. Thus, the kurtosis of a seismogram is smaller than the reflectivity series (Figure 2.2).

2.3 Skewness

In statistics, skewness is a third-order statistic which measures the asymmetry of the probability of a real-valued random variable. The skewness value can be positive or negative. Qualitatively, a negative skew indicates that the probability density function has a longer tail on the left side than the right side and the bulk of the values lie to the right of the mean. A positive skew indicates that the tail on the right side is longer than the left side and the bulk of the values lie to the left of the mean. A zero value, therefore, typically indicates a symmetric distribution (Figure 2.3).

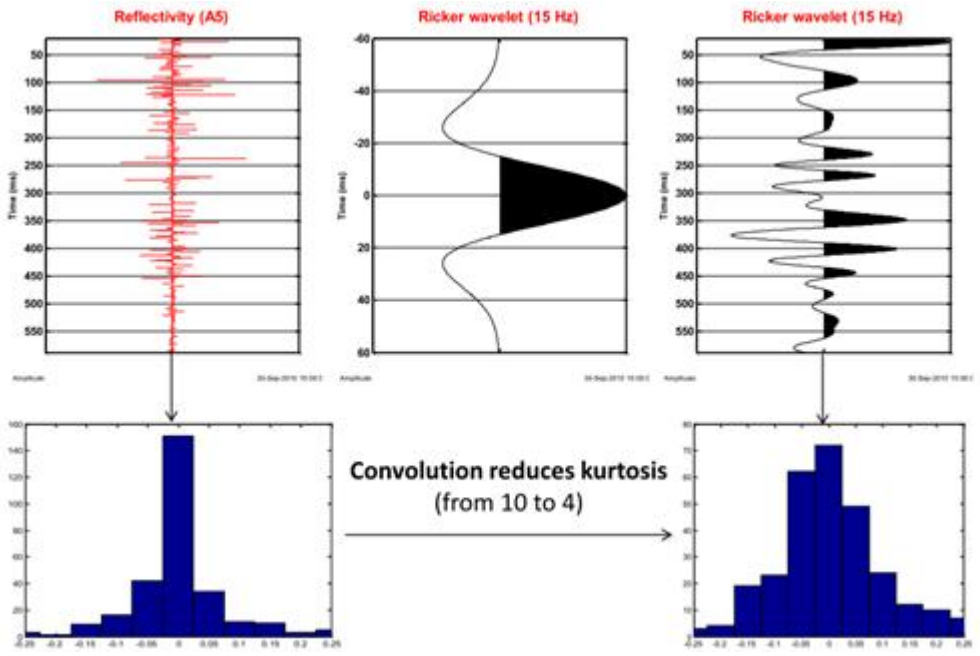

Figure 2.2: The amplitude distribution of seismogram is more Gaussian and has a smaller kurtosis compared to reflectivity series.

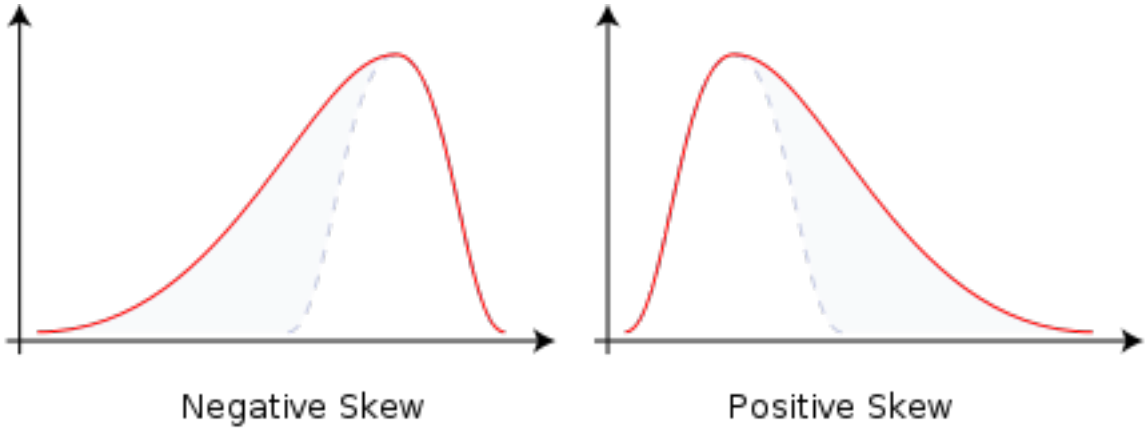

Figure 2.3: Negative skew has a longer tail on the left side and positive skew has a longer tail on the right side.

Chapter 3

Wavelet Phase Estimation Methods

Several wavelet phase estimation techniques have been proposed and studied. In this chapter, we discuss three different approaches: kurtosis phase estimation first developed by Wiggins (1978), recently studied by Van der Baan (2008) and Edgar (2008); a new phase estimation method developed in this thesis; and wavelet estimation through optimum Wiener filter. The theory, assumptions and limitations are described specific to each method of wavelet estimation tested.

3.1 Kurtosis Phase Estimation

3.1.1 Description and Theory

As previously described in section 2.2, the fourth-order statistic kurtosis holds information about the wavelet phase, therefore it could be used for wavelet estimation.

Based on the central limit theorem, the phase rotation which maximizes the kurtosis of the seismic amplitude distribution is the optimum wavelet phase.

First, a zero-phase wavelet is extracted from seismic data using the method described in section 2.1. The wavelength could be determined based on any a priori knowledge. Then a frequency-domain deconvolution is performed using an inverse filter as described in section 1.2.3. The deconvolution output, considered as inverted reflectivity is phase rotated in the time domain from -180 degrees to 180 degrees. The kurtosis after each rotation is extracted using equation 2.10. The phase rotation at the maximum kurtosis value is considered as the wavelet phase according to the central limit theorem. Therefore, the final wavelet is produced using the initial zero-phase wavelet amplitude spectrum, but with a phase rotation obtained from the maximum kurtosis scan.

3.1.2 Assumptions and Limitations

The most critical assumption of the Kurtosis Phase Estimation method is that a reflectivity series of the earth will have a super-Gaussian amplitude distribution so that maximizing the non-Gaussianity of the deconvolved output results in a more faithful representation of the subsurface geology. So the limitation of this method is that it is not applicable to near-Gaussian or Gaussian distributed reflectivity.

A further limitation of this method is that the polarity of the estimated wavelet is inherently ambiguous as it does not affect the kurtosis of the reflectivity. External control is required to determine the wavelet polarity.

The method requires a large amount of data for accurate kurtosis estimation. As

a high-order statistic, the kurtosis of a distribution needs to be determined from a large sample from the distribution.

3.2 Skewness for Polarity Determination

The polarity of a wavelet is a matter of convention. Here we use the SEG standard that for a zero-phase wavelet, a positive reflection coefficient is represented by a central peak. The caution is necessary since the European conventions are the opposite of the SEG standard.

As discussed in the last section, external information is needed to determine the polarity of the wavelet. It is found that the third-order statistic skewness could be used for wavelet polarity determination. Two synthetic seismograms produced by convolving the same reflectivity with two wavelets that have opposite polarity will have opposite skewness. So when the reflectivity is given, a synthetic seismogram is constructed by convolving estimated wavelet with reflectivity. Then the skewness of the synthetic seismogram is compared to the skewness of the real seismic data. If they have skewness with the same sign, i.e. either positive or negative, the polarity of the estimated wavelet is correct. If not, the polarity of the wavelet needs to be reversed.

3.3 Histogram Matching Phase Estimation

3.3.1 Description and Theory

This new method of wavelet estimation is based on the assumption that the optimum wavelet phase is that which makes the inverted reflectivity amplitude distribution have a better match with known reflectivity distribution. The use of the histogram matching, rather than kurtosis, has the immediate advantage that it does not require a super-Gaussian amplitude distribution for reflectivity.

Similarly to the KPE method, this method starts with zero-phase wavelet estimation. Then the frequency-domain deconvolution is performed in a bandwidth which contains the major part of wavelet energy (Figure 3.1). By doing this, the influence

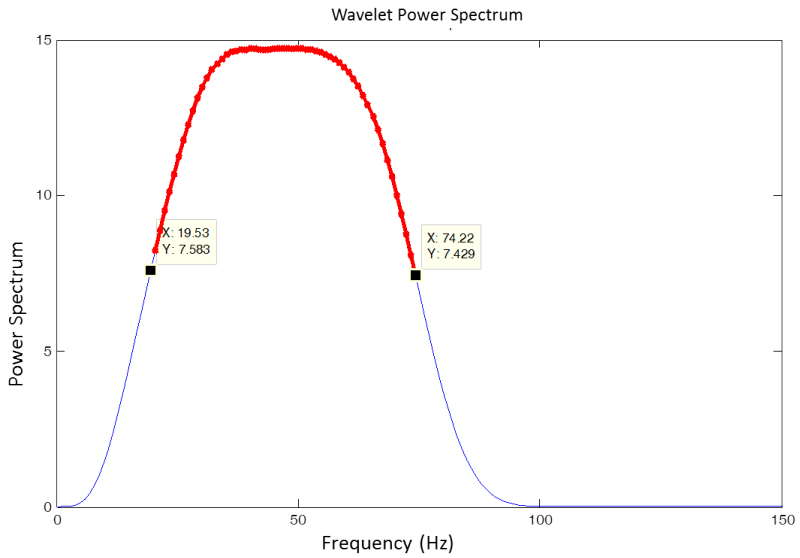

Figure 3.1: The frequency domain deconvolution is performed within a bandwidth containing major part of wavelet energy, as the red part shown in the wavelet power spectrum.

of the noise is reduced while enhancing the deconvolution output, thus increasing

the histogram match between inverted reflectivity and known reflectivity from well logs. The inverted reflectivity is phase rotated from -180 degrees to 180 degrees. The least-square error between histograms of inverted reflectivity with observed reflectivity histograms in wells after each rotation is calculated and a graph of the error variation with phase rotation is produced. The phase rotation at the minimum error value is the optimum wavelet phase.

3.3.2 Assumptions and Limitations

The histogram matching method assumes that a major part of the difference between inverted reflectivity amplitude distribution with observed reflectivity amplitude distribution is caused by the incorrect phase of wavelet. The reflectivity series is assumed to be white so the wavelet amplitude spectrum could be well determined by the average amplitude spectra of all wavelets in all traces of the input seismogram. In this case, the wavelet is assumed to be stationary in time and spatially invariant.

3.4 Optimum Wiener Filter Wavelet Estimation

3.4.1 Description and Theory

As described in Section 1.2.4, the optimum Wiener filter could be designed to minimize the least-square error between the actual and desired output. So the wavelet could be considered as a filter that minimizes the difference between the reflectivity series and input seismogram. Given the reflectivity from well logs and real seismic data, the wavelet could be estimated by solving the normal equation (equation 1.6).

Unlike the previously discussed two methods, this method estimates the wavelet in a one-step procedure instead of separating it into phase and amplitude.

3.4.2 Assumptions and Limitations

One critical limitation of this method is that it requires a perfect timing match between the input and desired output. In other words, if a wrong timing relationship exists between the reflectivity series and seismogram, the estimated wavelet could be significantly deviated from the true wavelet. This wrong timing relationship could be easily introduced by small errors in the well or seismic datum, or a systematic error in the check-shot measurements.

Similar to the other two methods, the wavelet is assumed to be stationary in time and spatially invariant. The noise in seismic data is considered to be negligible. The convolutional model is assumed to be valid.

Chapter 4

Results and Discussions

The three wavelet estimation methods are tested on different data sets. The first part of this chapter describes the implementation processes specific to each method of wavelet phase estimation tested. It aims to illustrate the work flow of each method. Of particular importance to the interpretation of the results are the assumptions and limitations of each method, thus special data sets are designed to justify their presentation in the second part.

4.1 Implementation and Program Testing

The data set used in this section is a synthetic trace (Figure 4.3) generated by the convolutional model. The reflectivity is from a random number generator and follows a Laplace distribution (Figure 4.2). The wavelet is 20Hz Ricker wavelet and phase rotated by 30 degrees (Figure 4.1). Wavelength is 120ms and the trace length is 2s with 2ms sampling rate.

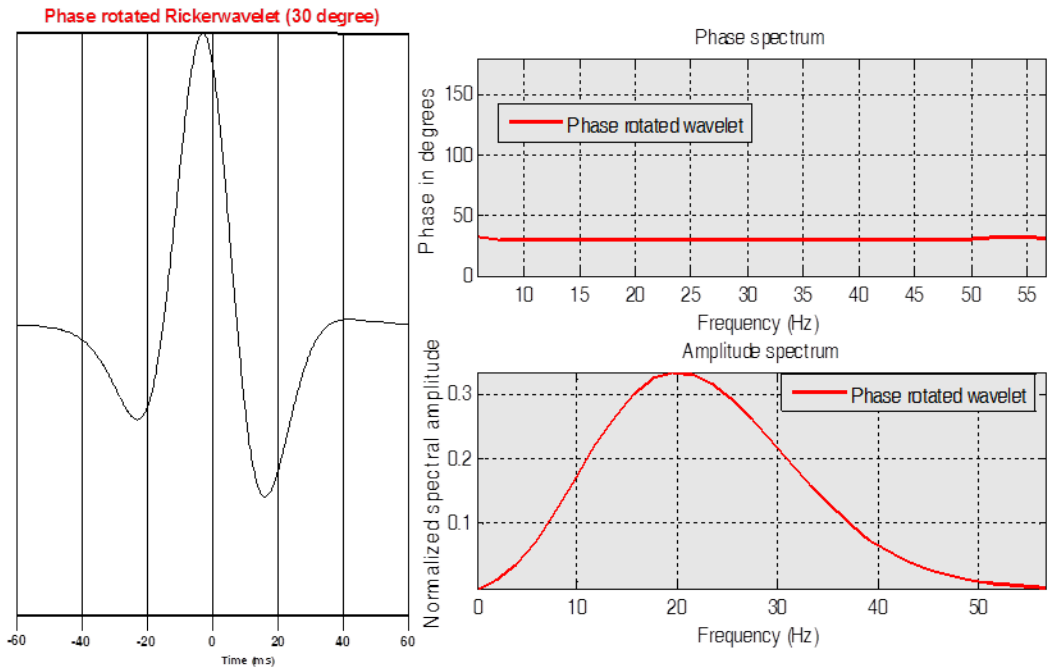

Figure 4.1: Ricker wavelet used in convolutional model.

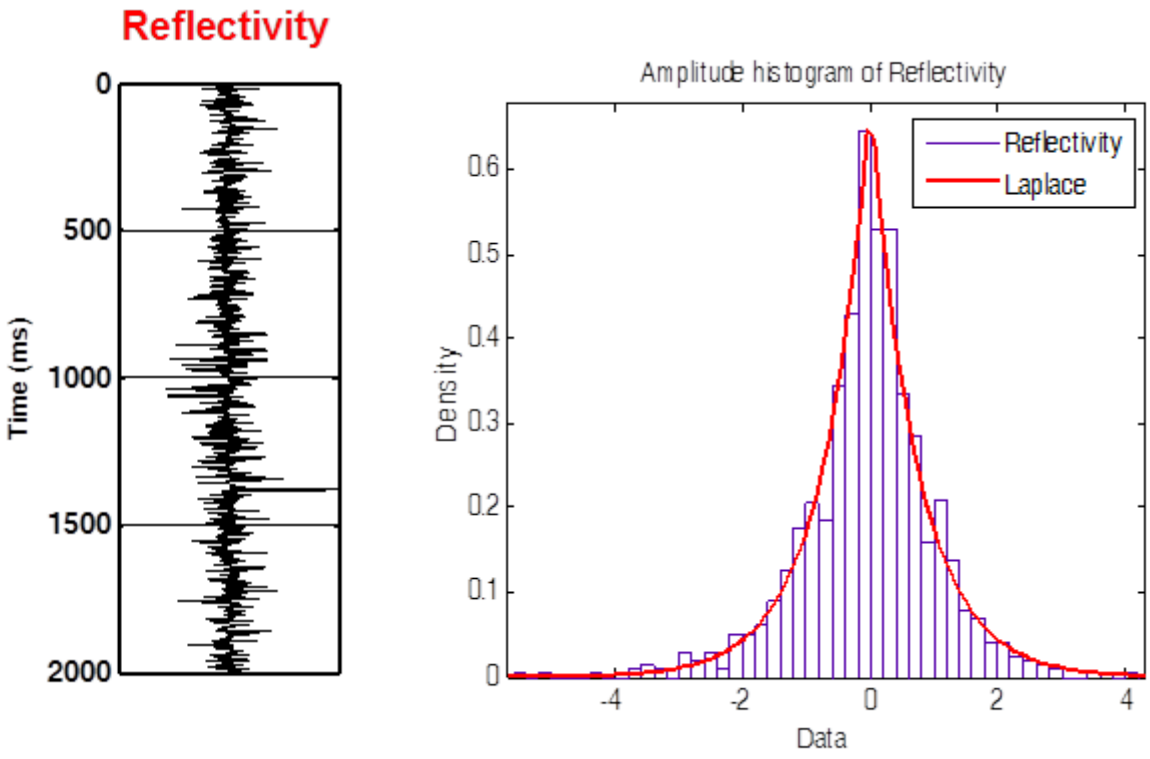

Figure 4.2: Reflectivity generated by Laplacian random number generator.

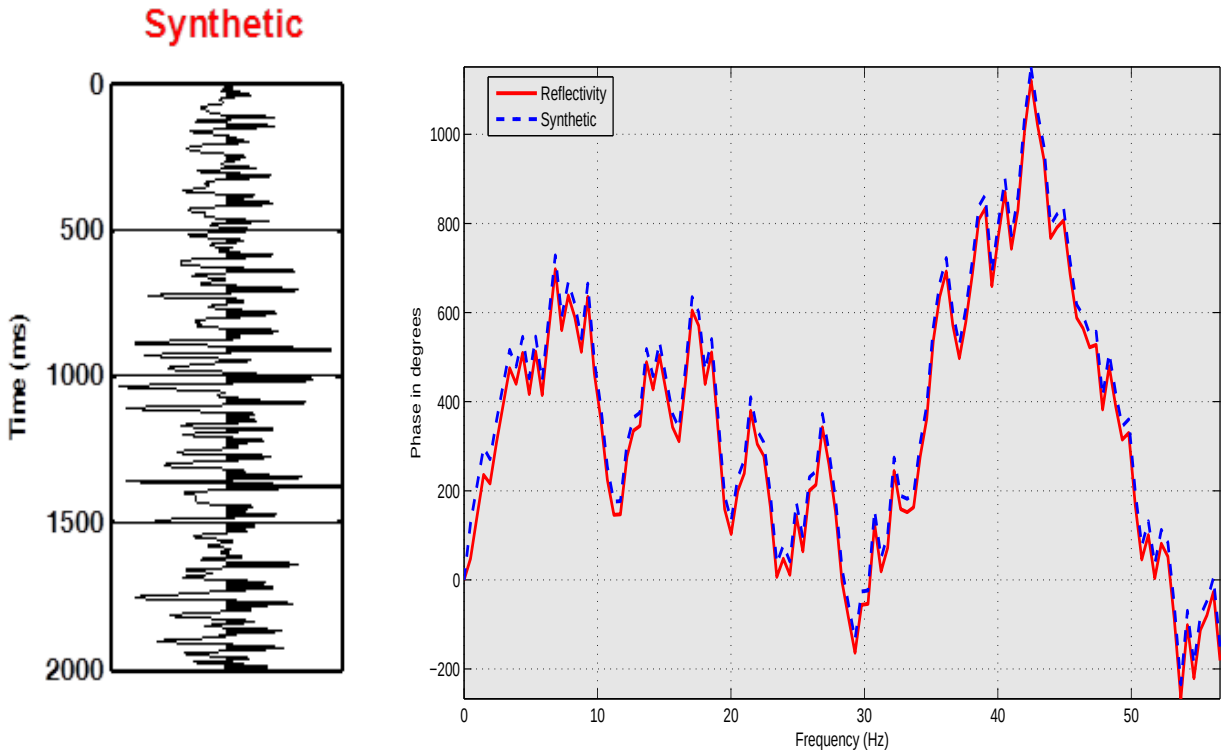

Figure 4.3: Theoretical synthetic trace by convolving wavelet with reflectivity. Phase spectrum shows a 30 degrees difference between reflectivity and synthetic trace.

4.1.1 Kurtosis Phase Estimation

First the zero-phase wavelet is extracted from seismic data using the method described in section 2.1 (Figure 4.4).

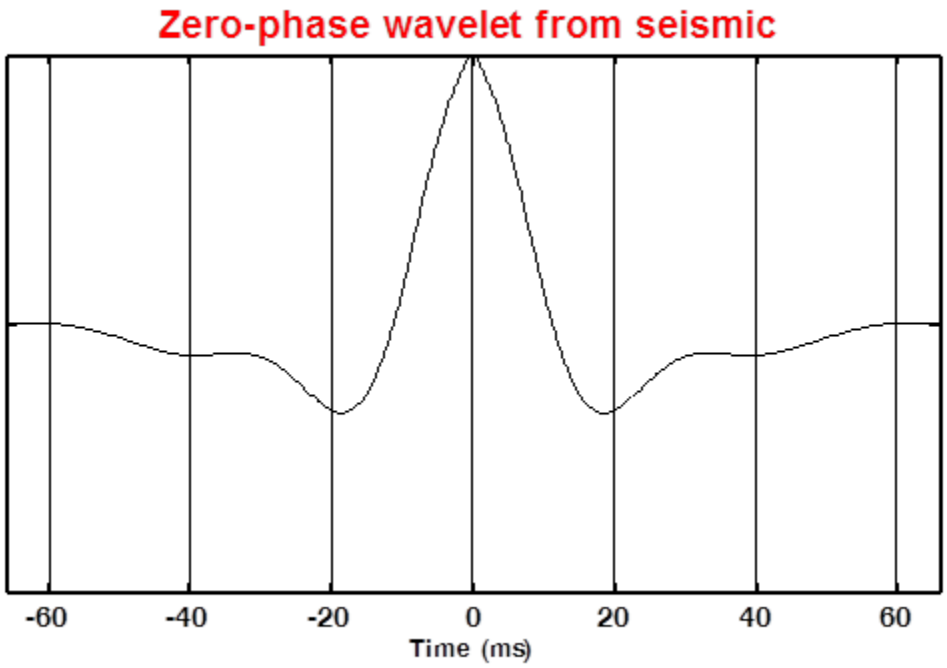

Figure 4.4: Estimated zero-phase wavelet from seismic data.

Extracted zero-phase wavelet is deconvolved from seismic data to get inverted reflectivity (Figure 4.5). The inverted reflectivity is phase rotated in the time domain from -180 degrees to 180 degrees. The kurtosis after each rotation is extracted (Figure 4.6). The phase rotation at the maximum kurtosis value is considered as the wavelet phase. The final wavelet is produced using the initial zero-phase wavelet amplitude spectrum, but with a phase rotation obtained from the maximum kurtosis scan (Figure 4.7).

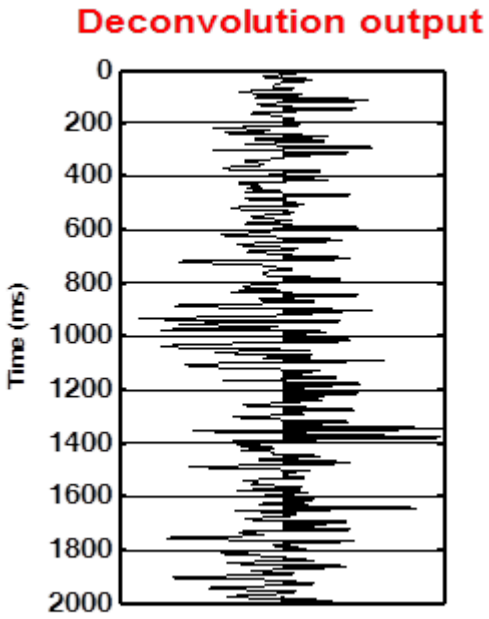

Figure 4.5: Deconvolution output using inverse filter in frequency domain.

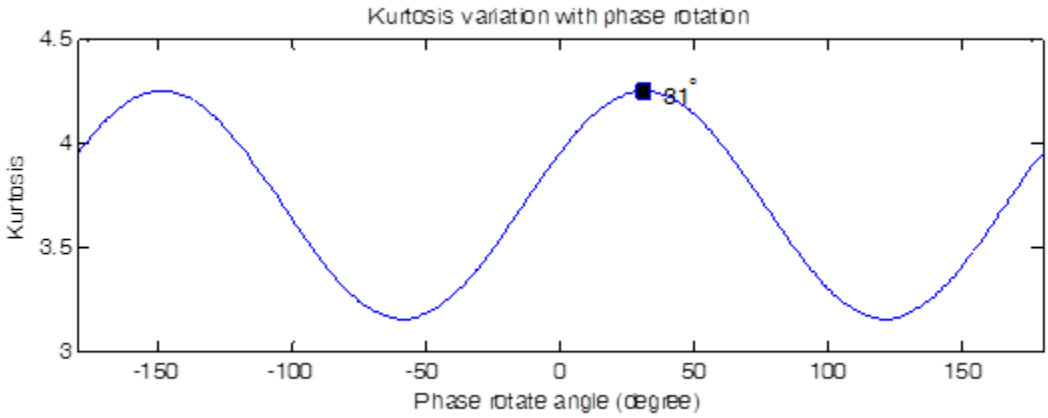

Figure 4.6: Kurtosis after each rotation is extracted using equation 2.10. The kurtosis reaches maximum at 31 degrees which corresponds to the wavelet phase. Notice that another maximum point appears at -149 degrees with a reverse polarity.

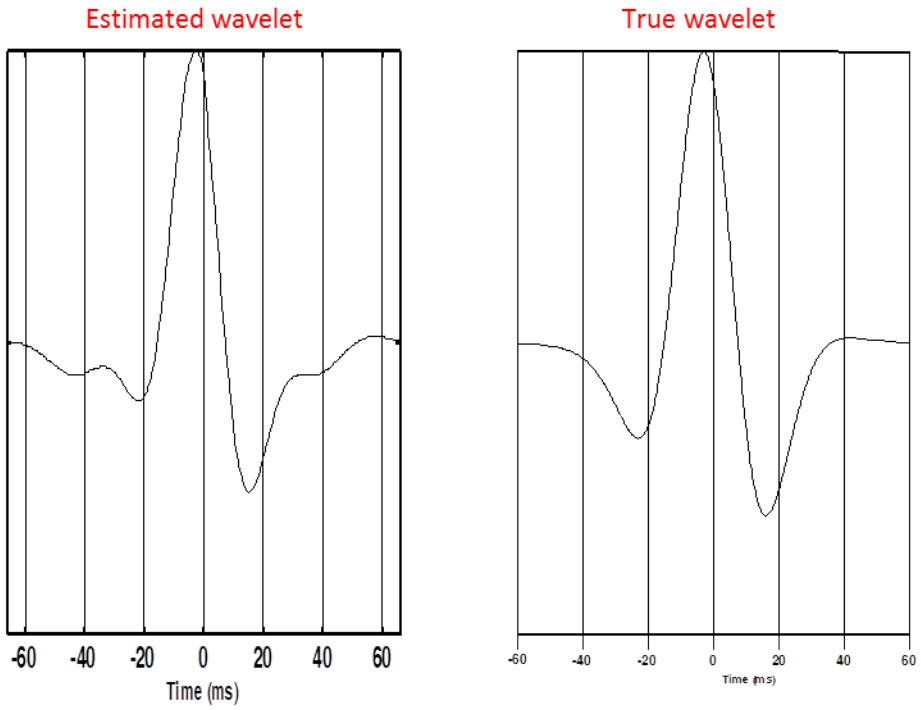

Figure 4.7: The comparison between the final estimated wavelet and true wavelet.

4.1.2 Histogram Matching Phase Estimation

First the zero-phase wavelet is extracted from seismic data. The bandwidth chosen for frequency-domain deconvolution is set so that the energy contained in the bandwidth is larger than a quarter of maximum power (Figure 4.8). Other frequency components are zeroed out.

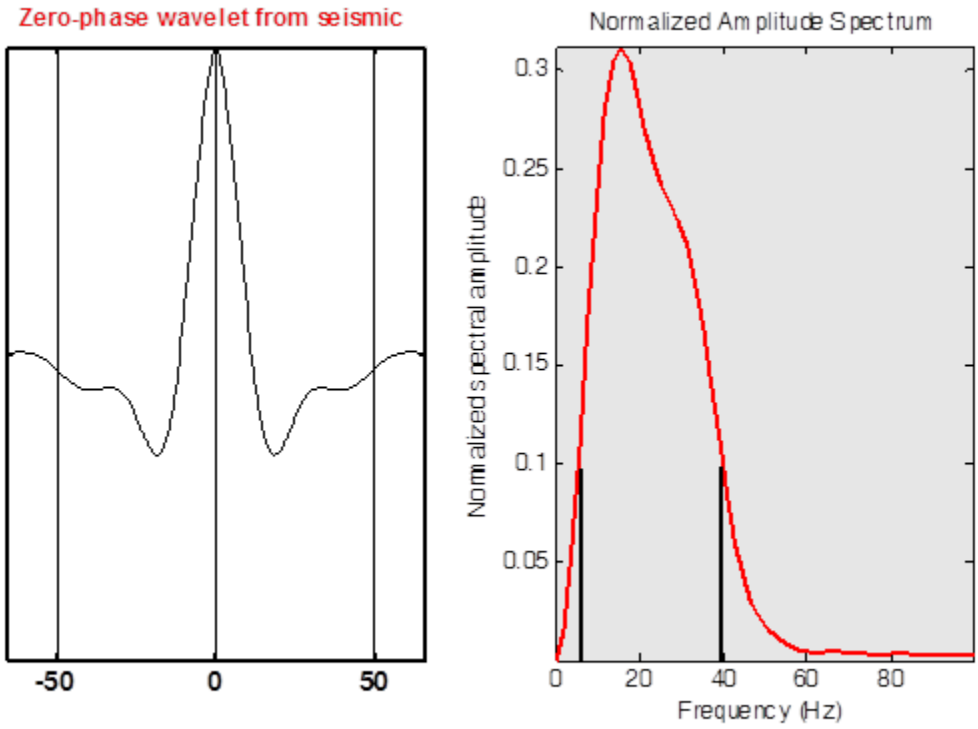

Figure 4.8: The Zero-phase wavelet is extracted from seismic data. Frequency-domain deconvolution is performed within a bandwidth where energy is larger than one quarter of maximum power indicated by vertical lines in the amplitude spectrum.

After deconvolution, the frequency components out of deconvolution bandwidth for reflectivity are also zeroed out to obtain narrow-band reflectivity (Figure 4.9).

After we get inverted reflectivity from deconvolution and narrow-band reflectivity, the amplitude histogram of narrow-band reflectivity is fitted using the kernel

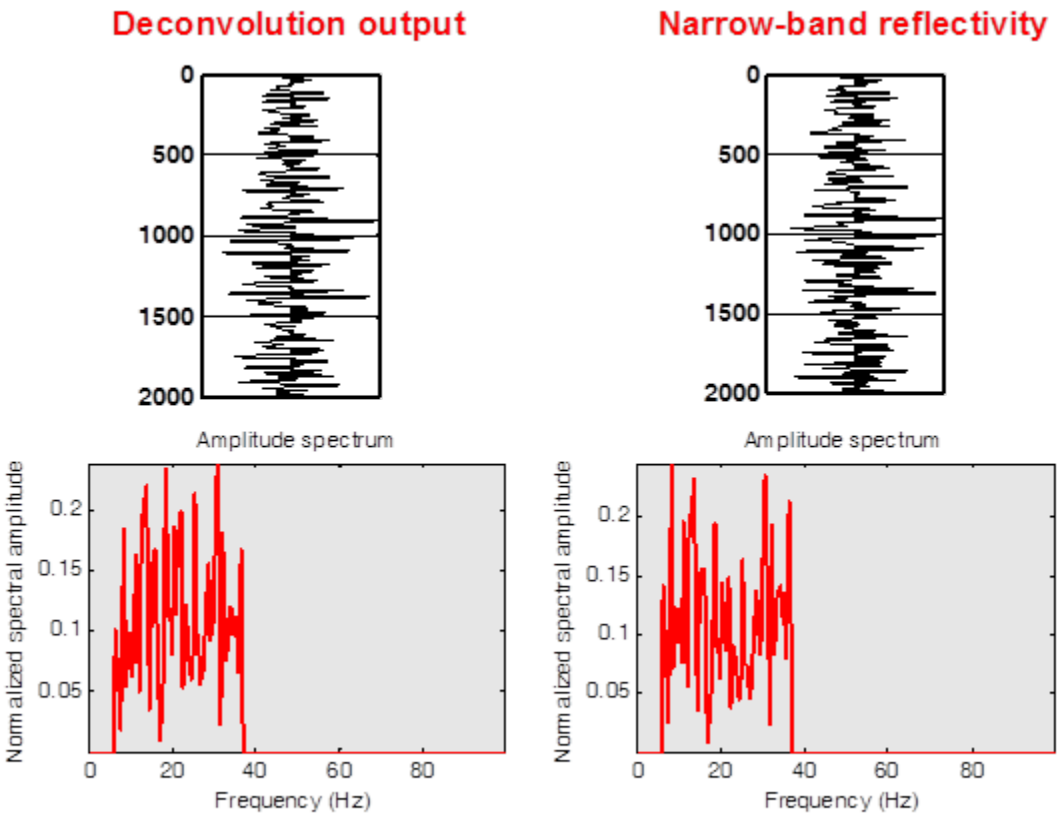

Figure 4.9: For both deconvolution output and reflectivity, frequency components outside of deconvolution bandwidth are zeroed out.

smoothing density estimate (Figure 4.10). The inverted reflectivity is phase rotated from -180 degrees to 180 degrees. The least-square error between the amplitude histogram of phase-rotated inverted reflectivity and the fit of narrow-band reflectivity's histogram is calculated and a graph of the error variation with phase rotation is produced (Figure 4.11).The comparison between estimated wavelet by histogram matching and true wavelet is shown in Figure 4.12.

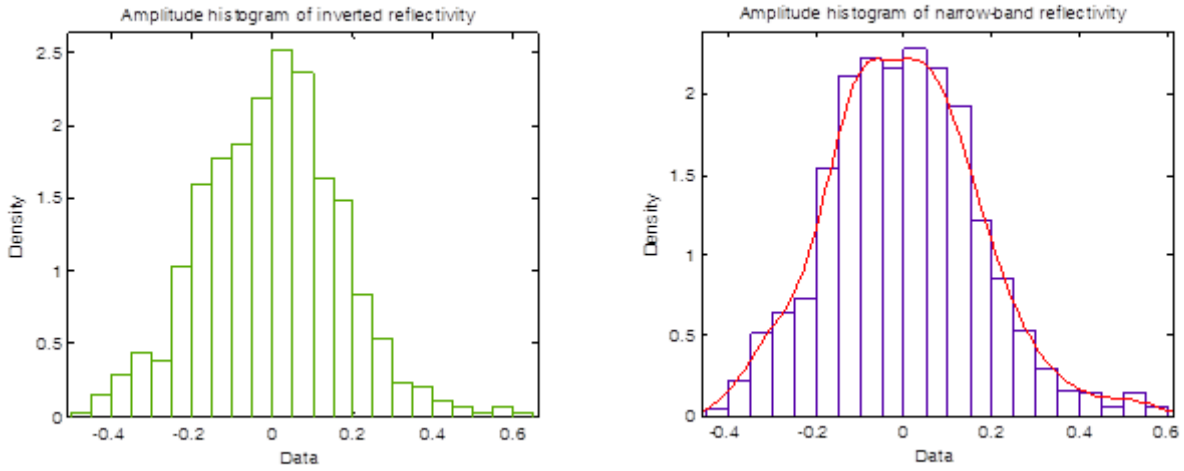

Figure 4.10: The amplitude histogram of narrow-band reflectivity is fitted using the kernel smoothing density estimate. These two histograms are compared to find the phase of the wavelet.

4.1.3 Optimum Wiener Filter Wavelet Estimation

As described in section 3.4.1, given the reflectivity and seismic data, the wavelet could be estimated as a match filter which matches reflectivity and seismic data in the least squares sense (Figure 4.13).

Notice that the optimum Wiener filter wavelet estimation is nearly perfect. This

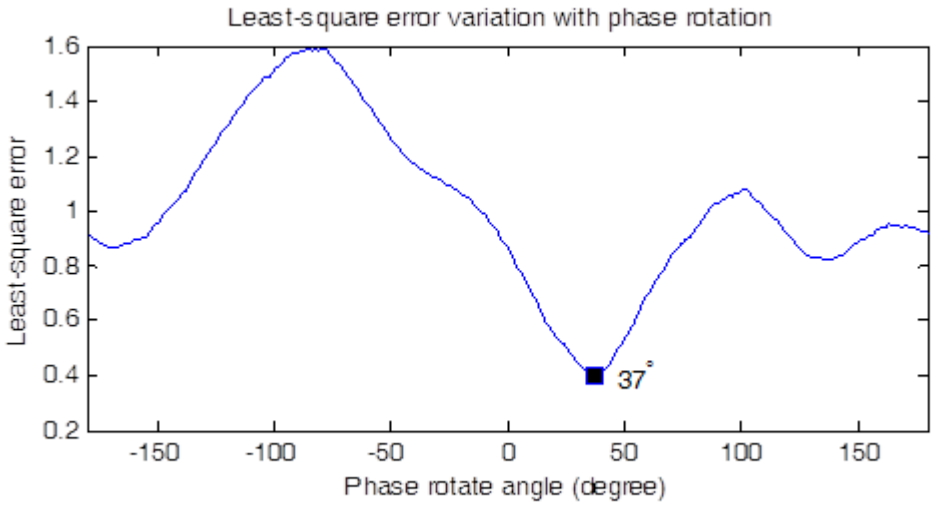

Figure 4.11: The least-square error between histograms of inverted reflectivity with observed reflectivity histograms in wells after each rotation is calculated. The minimum error is found at 37 degrees which is close to the true phase 30 degrees.

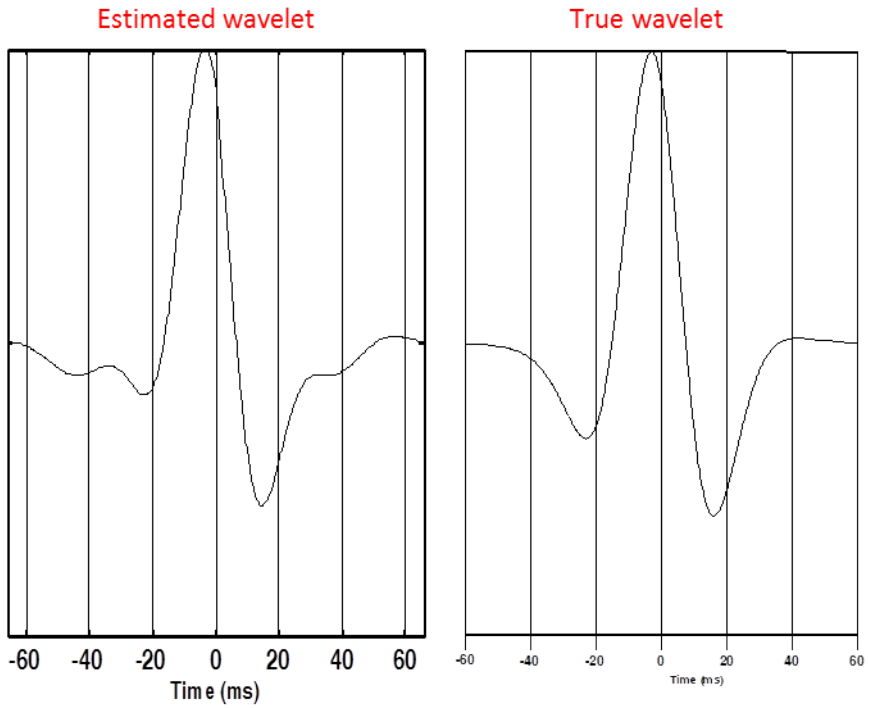

Figure 4.12: The comparison between estimated wavelet by histogram matching and true wavelet.

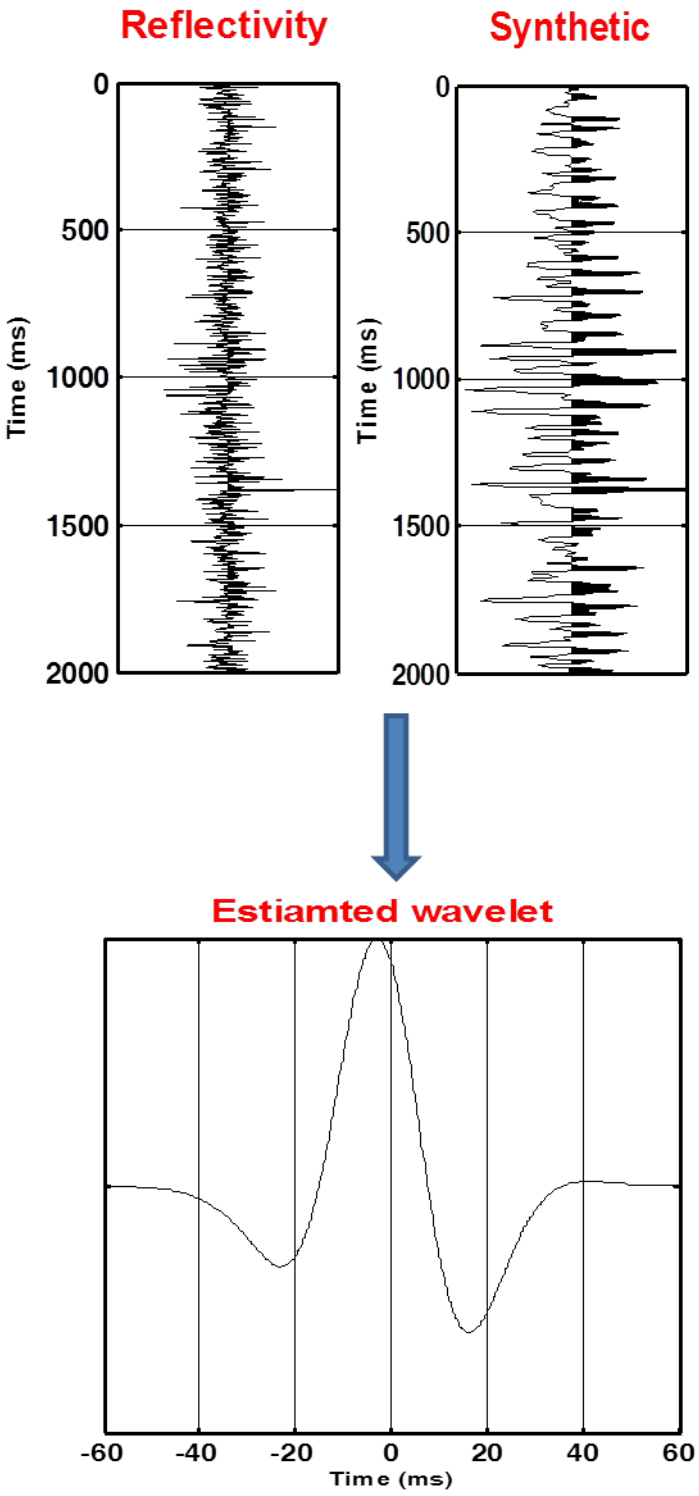

Figure 4.13: Optimum Wiener filter wavelet estimation.

is because the synthetic trace is created by the convolutional model and no noise is considered.

4.2 Limitations and Assumptions Test

First a Gaussian distributed reflectivity series is generated using a random number generator. A synthetic trace is constructed based on the convolutional model (Figure 4.14).

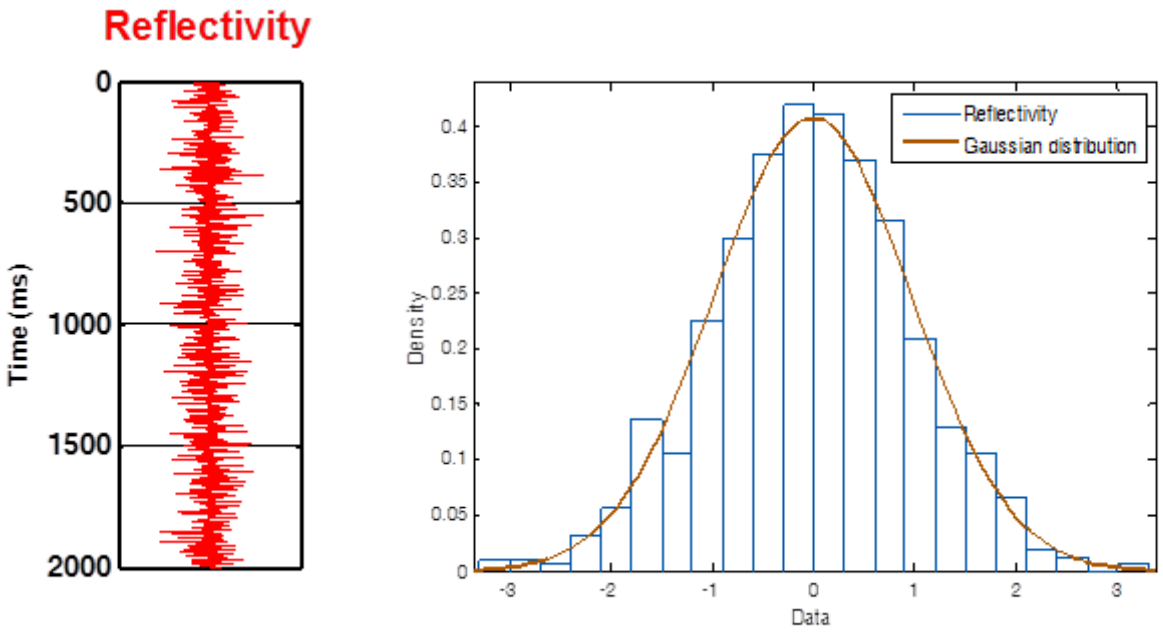

Figure 4.14: Gaussian distributed reflectivity from random number generator.

A 90 degree phase-rotated Ricker wavelet is used to construct synthetic trace (Figure 4.15). Estimated wavelets using three different methods are shown below:

It is noticed that the Kurtosis phase estimated wavelet is far from the true wavelet

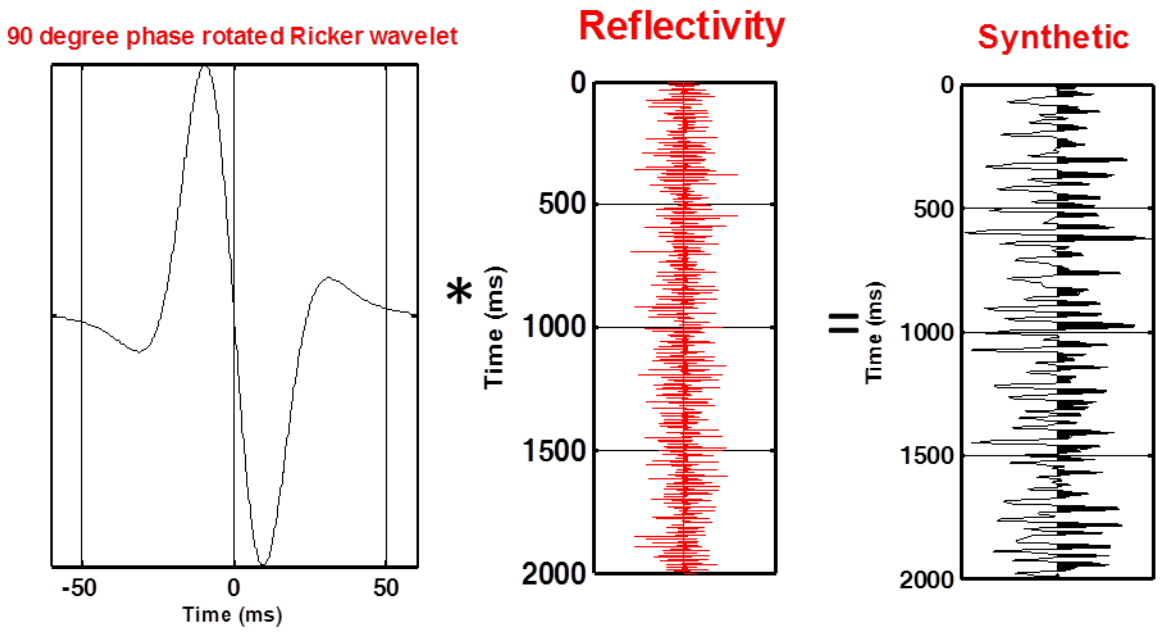

Figure 4.15: Synthetic trace is constructed using convolutional model.

due to the Gaussian distributed reflectivity. The other two methods can still give reasonable phase estimation.

Secondly, the same data set is used but a 20ms-time shift in synthetic trace is introduced (Figure 4.16). Estimated wavelets using three different methods are shown below:

Because of the inaccurate timing relationship between reflectivity and seismic data, optimum Wiener filter cannot estimate wavelet accurately. In both cases, the wavelet estimated using the method of histogram matching has good agreement with the true wavelet.

Furthermore reflectivity observed from 10 different wells are used to test these three methods on more realistic cases. Here shows one example from well A4. A 90-degree wavelet is used in the convolutional model (Figure 4.17). Estimated wavelets

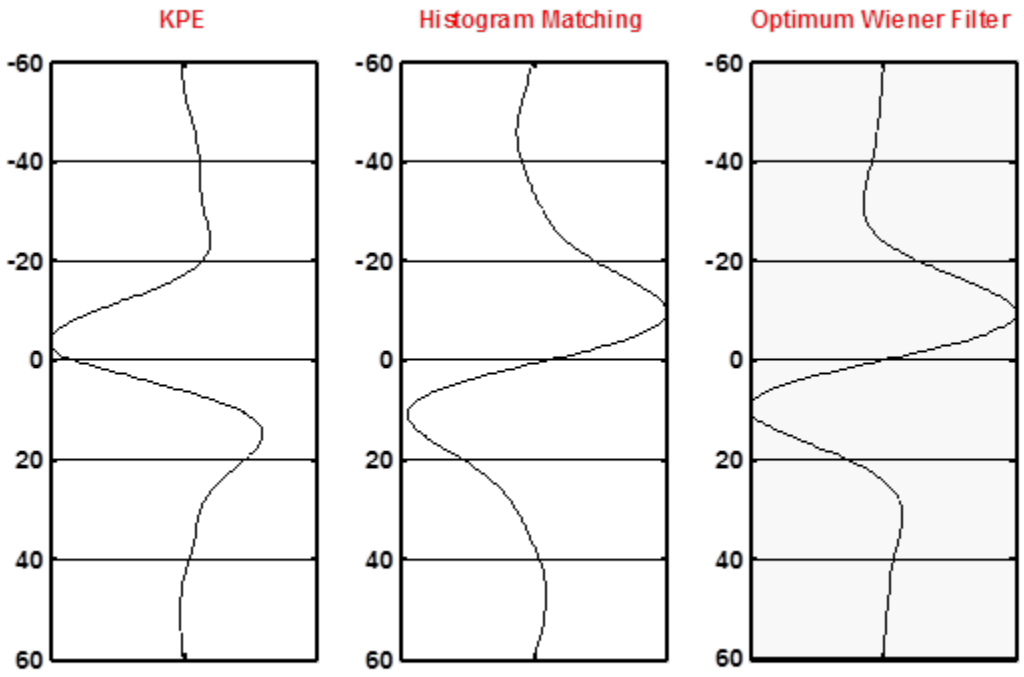

Figure 4.16: Comparison of wavelet estimation results on Gaussian distributed reflectivity.

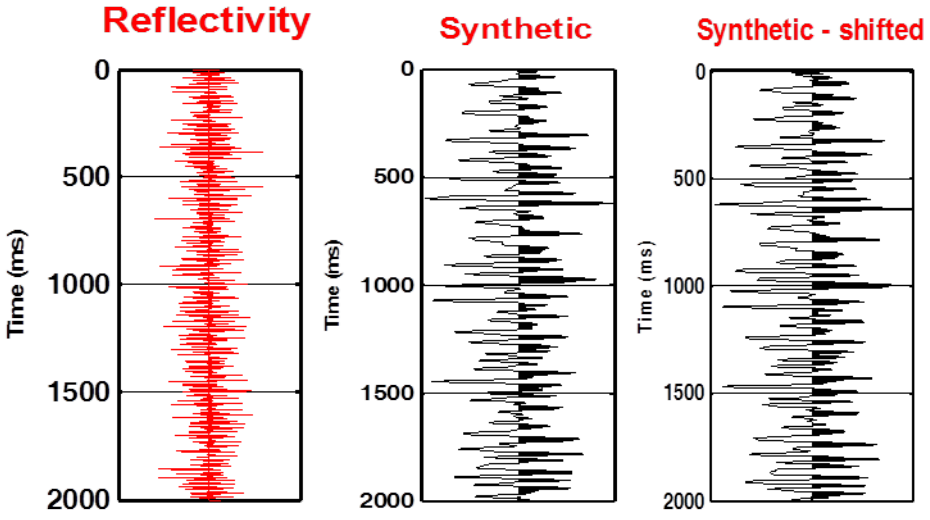

Figure 4.17: A 20ms-time shift is introduced to synthetic trace to simulate the situation with a wrong time-depth conversion.

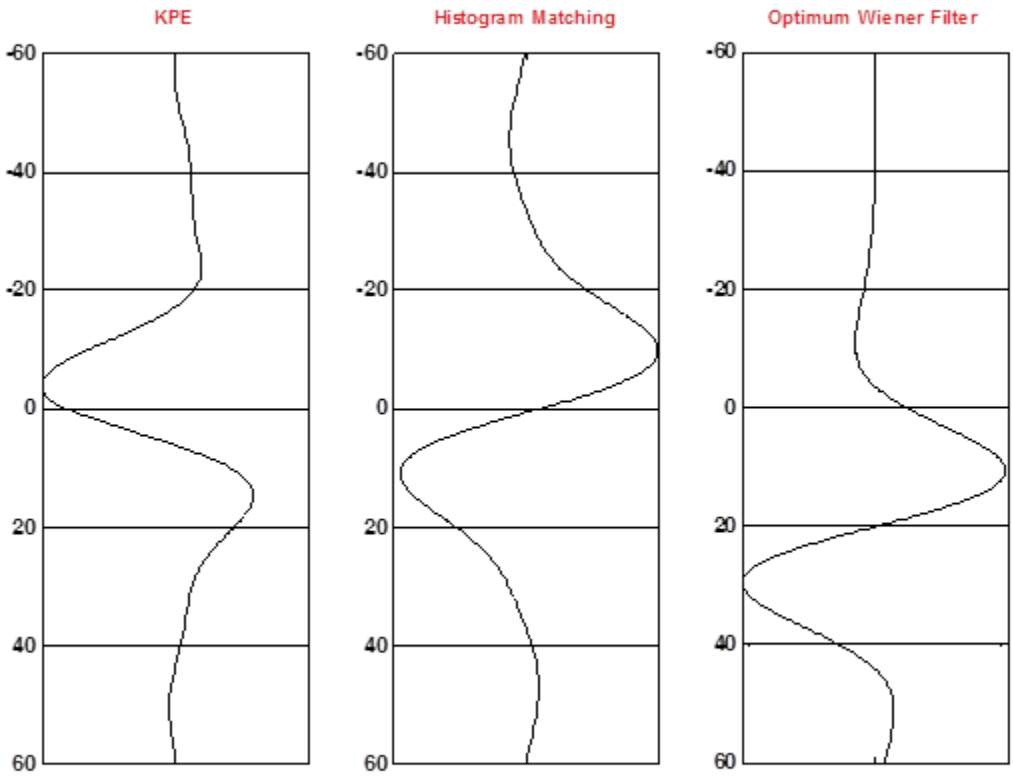

Figure 4.18: Comparison of wavelet estimation results on time shifted synthetic trace.

using three different methods are shown in figure 4.18. It is clear from visual inspections that there is good agreement between the true wavelet and estimated wavelets using histogram matching and optimum Wiener filter. But a large phase discrepancy exists between the kurtosis phase estimated wavelet and the true wavelet.

Table 4.1 shows all the wavelet phase estimation results using the histogram matching method in ten wells. Except for well A3, there is good agreement between the estimated wavelets and true wavelets. A phase difference less than 20 degrees is hard to see with the naked eye.

The poor performance of kurtosis phase estimation may be caused by insufficient data. To validate it, further tests are conducted on kurtosis phase estimation. We use synthetic traces with time length 2s, 4s, and 8s respectively. The sampling rate is 2ms for all traces. For each time length, 100 synthetic traces are randomly generated using the Laplace random number generator. The true phase of the wavelet is 90 degrees. The result is shown in Figure 4.19. It is noticed that, with an increasing time length, the accuracy of kurtosis phase estimation increased. For time length 2s, only 57 percent of phase estimation has an error of less than 20 degrees. For time length 4s, it increased to 60 percent and 74 percent for time length 8s.

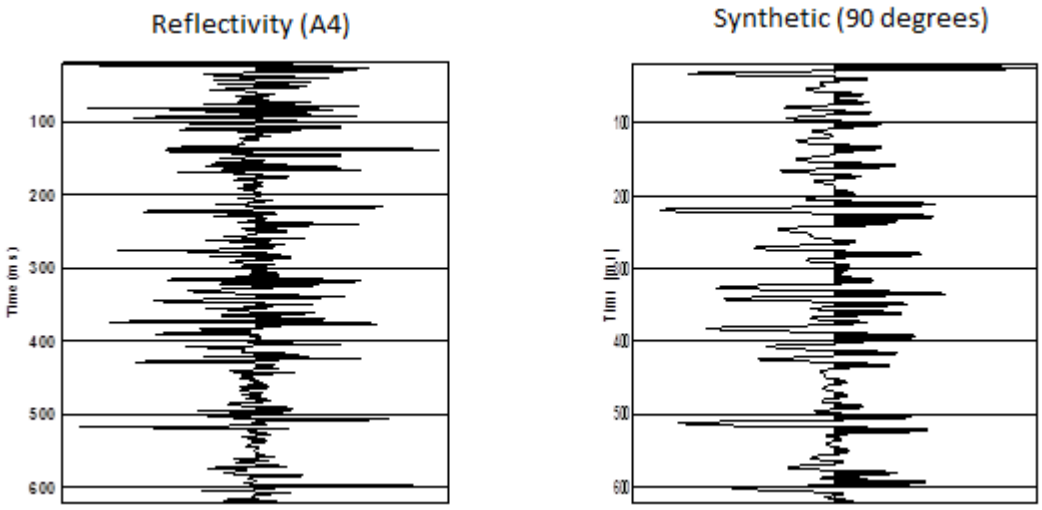

Figure 4.19: Reflectivity from well logs and synthetic traces using 90-degree wavelet.

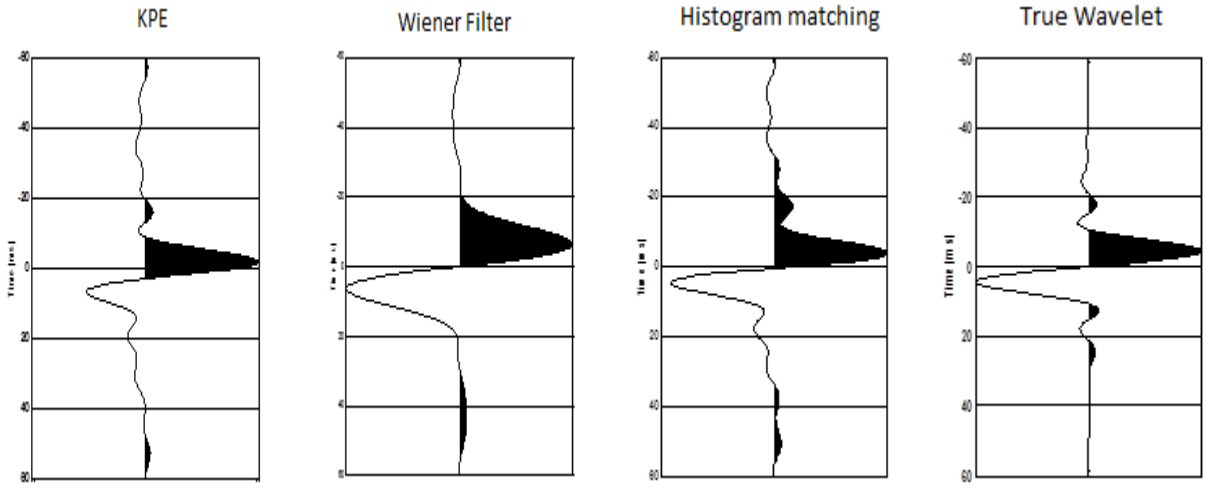

Figure 4.20: The comparison of true wavelet and estimated wavelet using three different methods. Notice that a large phase discrepancy exists between the true wavelet and the KPE estimated wavelet.

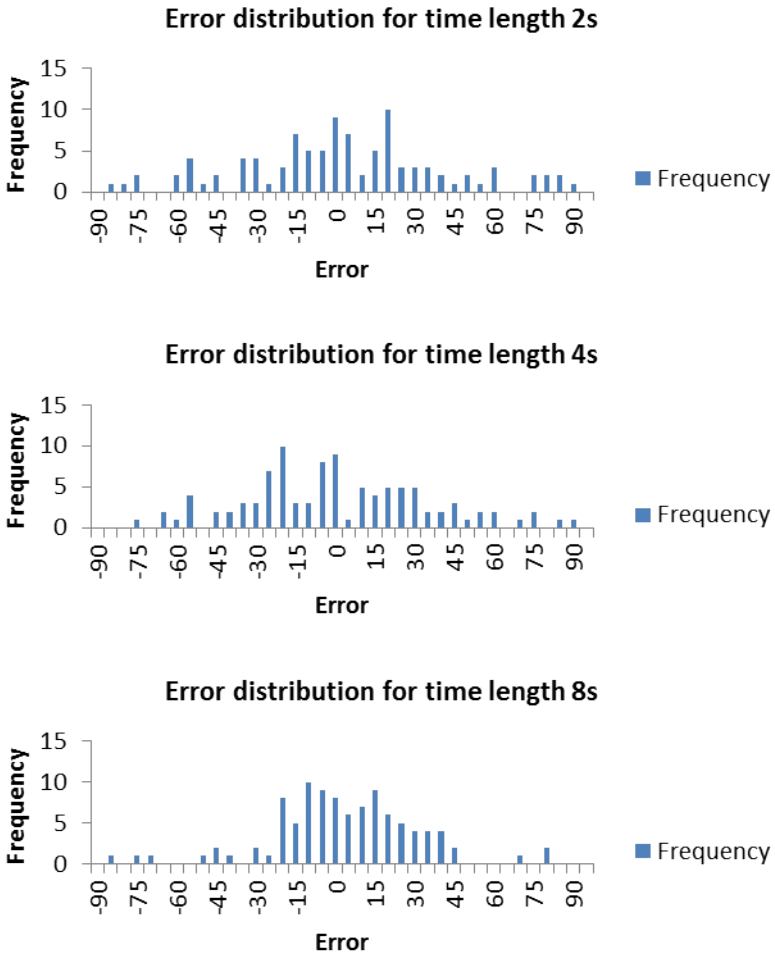

Figure 4.21: With an increasing time length, the errors for phase estimation are more confined within 20 degrees.

Histrogram Matching (True phase: 90 degrees)		
Well	Estimated phase	Error
A1	75	15
A2	103	13
A3	**44**	**46**
A4	83	7
A5	85	5
A6	83	7
A9	86	4
B1	108	18
B2	93	3
B3	109	19

Table 4.1: Results of phase estimation using histogram matching for 10 different wells. The true phase is 90 degrees. Except well A3, all estimated phase have errors of less than 20 degrees.

Chapter 5

Conclusions

Seismic wavelet phase information is important to seismic data processing and interpretation. There are several wavelet phase estimation methods, including the kurtosis phase estimation method recently studied by Vander Baan et al. (2008) and the optimum Wiener filter. I developed and studied a new phase estimation method based on histogram matching. This method compares histograms of inverted reflectivity obtained using different wavelets having the same amplitude spectrum with observed reflectivity histograms in wells. The method gives accurate seismic wavelet phase estimation with an error of less than 20 degrees provided reflectivity distribution.

I tested the kurtosis phase estimation method, optimum Wiener filter wavelet estimation method and histogram matching phase estimation method on synthetic traces. Synthetic traces are built based on the convolutional model and both randomly generated reflectivity and well-extracted reflectivity are used. The histogram matching method successfully estimated the wavelet phase from synthetic traces

generated from Gaussian distributed reflectivity, Laplace distributed reflectivity and well-extracted reflectivity. A time shift between reflectivity and seismic traces does not affect phase estimation results. Random generated synthetic traces with three different time length (2s, 4s, 8s) are used to test the stability of kurtosis phase estimation. For each time length, 100 synthetic traces are created by convolution of the 90-degree Ricker wavelet and the reflection series, which is generated by the Laplace random number generator. For 2s-length traces, kurtosis phase estimation can estimate phase with error less than 20 degrees for only 57 of 100 tests. For 4s-length traces, this number increases to 60 out of 100, and 74 out of 100 for the 8s-length traces. When a perfect timing relationship is given between reflectivity and synthetic traces, the optimum Wiener filter could estimate the wavelet nearly identical to the true wavelet. However, a 20ms second time shift significantly lowers the accuracy of phase estimation. The model tests also show that a white reflectivity generated by a random number generator provides a better phase estimation since the amplitude spectrum of the wavelet is well estimated. However, the histogram matching method is insensitive to the polarity of the data. Thus, the polarity is determined from the skewness of the inverted distribution.

Bibliography

Ansey, N. A., 1958, Why all this interest in the shape of the pulse?: Geophysical Prospecting, **6**, 394–403.

Badley, M., 1985, Practical seismic interpretation: International Human Resources Development Corporation.

Brown, A., 2004, Interpretation of three-dimensional seismic data: American Association of Petroleum Geologists and the Society of Exploration Geophysicists.

Edgar, J. A., 2008, A Comparison of Seismic Wavelets Derived using Statistical Wavelet Estimation Techniques and Deterministic Seismic-to-Well Ties: Master's thesis, University of Leeds.

Halmos, P. R., 1944, The foundations of probability: The American Mathematical Monthly, **51**, pp. 493–510.

Liner, C. L., 2002, Phase, phase, phase: The Leading Edge, **21**, 456–457.

———, 2004, Elements of 3d seismology: PennWell.

Longbottom, J., A. T. Walden, and R. E. White, 1988, Principles and application of maximum kurtosis phase estimation1: Geophysical Prospecting, **36**, 115–138.

Robinson, E. A., 1957, Predictive decomposition of seismic traces: Geophysics, **22**, 767–778.

Sacchi, M. D., and T. J. Ulrych, 2000, Nonminimum-phase wavelet estimation using higher order statistics: The Leading Edge, **19**, 80–83.

Sheriff, R. E., 2002, Encyclopedic dictionary of applied geophysics, fourth ed.: Society of Exploration Geophysicists.

Simm, R., and R. White, 2002, Tutorial: Phase, polarity and the interpreter's wavelet: First Break, **20**, 277–281.

Treitel, S., and E. A. Robinson, 1967, Intoduction: special issue on the m.i.t. geophysical analysis group reports: Geophysics, **32**, 415–417.

van der Baan, M., 2008, Time-varying wavelet estimation and deconvolution by kurtosis maximization: Geophysics, **73**, V11–V18.

van der Baan, M., and S. Fomel, 2009, Nonstationary phase estimation using regularized local kurtosis maximization: Geophysics, **74**, A75–A80.

van der Baan, M., S. Fomel, and M. Perz, 2010, Nonstationary phase estimation: A tool for seismic interpretation?: The Leading Edge, **29**, 1020–1026.

van der Baan, M., and D. Pham, 2008, Robust wavelet estimation and blind deconvolution of noisy surface seismics: Geophysics, **73**, V37–V46.

White, R. E., and P. N. S. O'Brien, 1974, Estimation of the primary seismic pulse: Geophysical Prospecting, **22**, 627–651.

Wiggins, R. A., 1978, Minimum entropy deconvolution: Geoexploration, **16**, 21 – 35.

Yilmaz, Ö., 2001, Seismic data analysis: processing, inversion, and interpretation of seismic data: Society of Exploration Geophysicists.

Ziolkowski, A., 1991, Why don't we measure seismic signatures?: Geophysics, **56**,

190–201.